First publ. in: Materials Research Society Symposium Proceedings 407 (1996), pp. 167-172

STRUCTURAL RELAXATIONS IN A SIMPLE MODEL MOLTEN SALT

Matthias Fuchs
Department of Materials Science, University of Illinois, Urbana, Il 61801

Abstract

The structural relaxations of a dense, binary mixture of charged hard spheres are studied using the Mode Coupling Theory (MCT). Qualitative differences to non–ionic systems are shown to result from the long–range Coulomb interaction and charge ordering in dense molten salts. The presented non–equilibrium results are determined by the equilibrium structure, which is input using the well studied Mean Spherical Approximation.

Introduction

The equilibrium structure of ionic liquids is strongly affected by the long–range nature of the Coulomb interaction [1]. One aspect is the screening of external charges familiar from the Debye-Hückel theory of ionic solutions. Another aspect are oscillations in the charge density around a given ion. These oscillations result from the competition between local charge neutrality and the excluded volume restriction due to the finite diameter of the ions. Also the dynamics of equilibrium ionic liquids in the hydrodynamic regime differs from the one of uncharged mixtures. Coulombic restoring forces lead to a non–diffusive and non–propagating relaxation of charge fluctuations [1]. The MCT determines the slow structural relaxations of dense (supercooled) liquids from their equilibrium structure [2]. In this paper we discuss the most salient features of these results arising from the long–range Coulombic interactions. These will be seen to be directly connected to the familiar effects in the static structure mentioned above: screening and charge ordering.

Theory

One of the most simple models of an molten salt is a binary mixture of hard spheres with radii d_i and charges z_i, $i = 1, 2$. Global charge neutrality fixes $z_1\varrho_1 + z_2\varrho_2 = 0$, where ϱ_i denotes the density of species i. The mean spherical approximation [3] gives a satisfactory description of the equilibrium structure of this system, which depends on the parameters d_1/d_2, z_1/z_2, packing fraction φ and coupling constant Γ. The packing fraction is the ratio of volume occupied by spheres to the total volume. Γ is a generalized inverse Debye screening length and a measure of the Coulomb interaction compared to the thermal energy. At the values of these parameters chosen in our study and collected in table I one observes a liquid to glass transition in the MCT equations. This transition is the topic of the work reported. It is worth noting that the density at the transition can be chosen to be lower than in the uncharged system [4]. Obviously, the charges increase the interactions of the particles. Asymmetric parameters ($d_1/d_2 \neq 1$) were first chosen in order to study experimentally more realistic non–symmetric salts. The charge asymmetry z_1/z_2, however, was then adjusted to obtain the value $\lambda = 0.85$ for the exponent parameter λ; see the discussion. The MCT for binary mixtures formulates a closed set of equations for the time and wave vector dependent density fluctuation functions, $F_q^{ab}(t) = \frac{1}{N}\langle\delta\varrho_q^{a*}(t)\delta\varrho_q^b(0)\rangle$ [5,2]. Of particular interest are the fluctuations of the total– or mass–, $\varrho^n = \varrho^1 + \varrho^2$, and the charge–density, $\varrho^c = z_1\varrho^1 + z_2\varrho^2$.

Table I: Molten salt equilibrium parameters and results from MCT calculation.

d_2/d_1	z_1/z_2	φ	Γ	$k_BT\epsilon d_2/e^2$	λ	b	γ	σ/τ	ε'_o	ε'_∞
1.2	-3	0.475	1.68	0.113 (from Γ)	0.845	0.40	3.24	0.49	14.9	3.56

The initial values, $F_q^{ab}(t=0) = S_q^{ab}$, are the static structure factors which are the only input determining the $F_q^{ab}(t)$ via the MCT equations.

MCT shows that these equations exhibit bifurcations which are identified as idealized liquid to glass transitions. Close to these transitions the long time dynamics is predicted to follow from

$$q^2 F_q(t) = S_q\{M_q(t)S_q - \frac{d}{dt}\int_0^t dt' M_q(t-t')F_q(t')\} \ , \tag{1}$$

where matrix notation is used and the memory functions are quadratic polynomials in the $F_q(t)$ correlators with coefficients determined by the static structure factors S_q [2,5]. Thermally activated transport is neglected in (1) leading to its breakdown at low temperatures. Only aspects which are not affected by this simplification will be discussed in this article.

Results

In order to screen an external charge the charge structure factor S_q^{cc} has to vanish for small q, $S_q^{cc} \propto (q\Lambda_D)^2$, where Λ_D is the Debye screening length [1,3]. This leads to a decoupling of the MCT equations (1) for small wave vector. Whereas the mass–density fluctuations are determined by a frequency dependent longitudinal viscosity $N^l(z=\omega+i\epsilon)$,

$$F_q^{nn}(z)/S_q^{nn} \to \frac{-1}{z - \frac{1}{S_0^{nn}N_0^l(z)}} \qquad \text{for } q\to 0, \text{ where} \qquad N_q^l(z) = \frac{1}{q^2}M_q^{nn}(z) \ , \tag{2}$$

the charge fluctuations couple to the generalized conductivity $\sigma(z)$

$$F_q^{cc}(z)/S_q^{cc} \to \frac{-1}{z + 4\pi i\sigma(z)} \qquad \text{for } q\to 0, \text{ where} \qquad \sigma(z) = \lim_{q\to 0}\frac{i}{4\pi}\frac{q^2}{S_q^{cc}M_q^{cc}(z)} \ . \tag{3}$$

These equations simplify further in two frequency windows reached close to a transition. From the well known MCT results let us only mention the von Schweidler decay which describes the onset of the α–relaxation, i.e. the final decay into equilibrium [2]:

$$F_q^{ab}(t)/S_q^{ab} = f_q^{ab} - h_q^{ab}\ (t/\tau)^b \qquad \text{for intermediate times} \ . \tag{4}$$

The von Schweidler exponent b and the exponent γ determining the increase of the α–relaxation time τ are functions of the exponent parameter λ and uniquely determined at the chosen transition. Their values are included in table I. Eq. (4) shows that the density fluctuations exhibit a two–step relaxation. The amplitudes f_q^{ab} of the final or α–relaxation is smaller than unity. The relaxation is non–exponential in general and the α–relaxation times τ_q^{ab} depend sensitively on temperature or density and on wave vector by a multiplicative factor, which roughly equals $(f_q^{ab}/h_q^{ab})^{1/b}$. The mass–density correlation functions qualitatively agree with the results obtained for neutral one–component liquids [2,6]. Fig. 1 shows the α–amplitudes, f_q^{nn}, which describe the frozen–in mass–density structure at the glass transition.

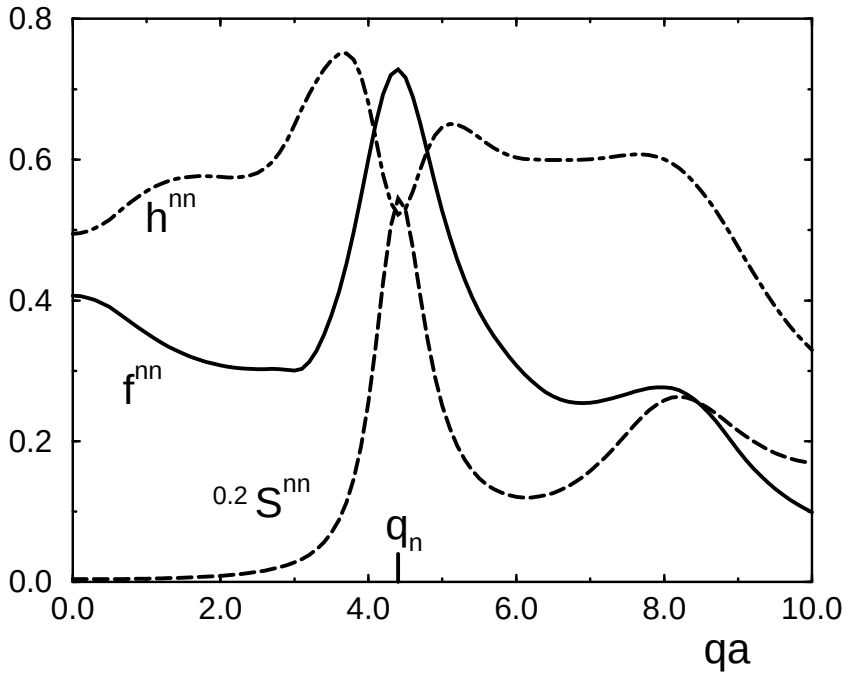

Figure 1: Mass–density α–amplitude f_q^{nn}, critical amplitude h_q^{nn} and structure factor S_q^{nn}.

The known local packing on shells separated by the mean average interparticle spacing, $a \approx q_n/4.4$, is seen in f_q^{nn} as a consequence of the one in S_q^{nn} [2,6]. Local neutrality and excluded volume effects lead to charge ordering and a prominent peak in the charge structure factor, S_q^{cc}. The average spacing between ion–shells of equal sign is larger than the average particle spacing resulting in the peak in S_q^{cc} to lie at q_c, where $q_c < q_n$. The charge–density fluctuations f_q^{cc}, which are arrested at the transition, reflect this ordering [4]; see Fig. 2.

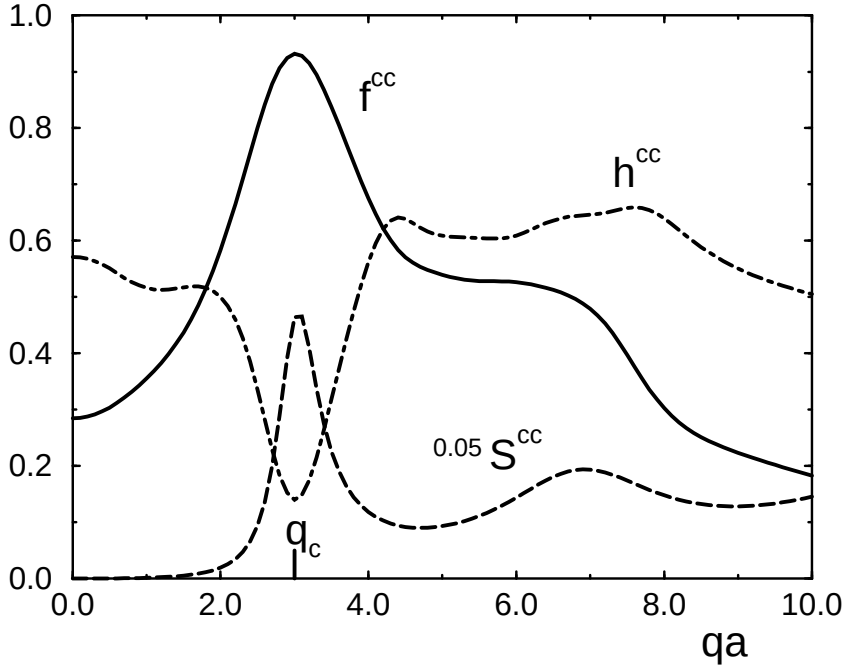

Figure 2: Charge–density α–amplitude f_q^{cc}, critical amplitude h_q^{cc} and structure factor S_q^{cc}.

The different mass– and charge–density ordering also leads to specific variations in the wave vector dependent prefactors of the α–relaxation times τ_q^{nn} and τ_q^{cc}. Fig. 3 shows these variations as estimated from the peak positions in the corresponding susceptibilities, $\tau\omega_{max} = 1$. A q–dependent slowing down at the maximal amplitudes of the α–process is observed. Superficially, this mimics the known De Gennes narrowing, as the τ_q vary in phase with the static structure factors [1]. However, this correlation only holds, because the α–relaxation amplitudes, f_q, vary in phase and the critical amplitudes, h_q, vary out of phase with the structure factors, S_q [2]; see Figs. 1 and 2.

The results presented thus far specify the structural relaxations on length scales of the order of interparticle distances. Analyzing Eq. (1) more closely, it is seen that it also is the static structure on these length scales which determines the results. The quantitative results therefore depend on the appropriateness of the underlying microscopic model, i.e. the liquid of charged hard spheres with the choice of parameters. From Eqs. (1,3) one can also obtain macroscopic transport coefficients like the conductivity σ and the dielectric constant ε' of the ionic melt. Their values are included in table I. The frequency dependent conductivity determines the dielectric "constant" via

$$\varepsilon(z) = 1 + 4\pi i \frac{\sigma(z)}{z} \; . \tag{5}$$

The liquid molten salt is characterized by a conductivity and dielectric constant measured at low frequencies, $\omega\tau \ll 1$. In the idealized glassy state the particles are arrested and ionic transport over macroscopic distances is not possible. The α–relaxation time τ diverges and the conductivity vanishes. Eq. (5) then results in a dielectric constant ε_∞ which can also be observed in the liquid state at high frequencies, $\omega\tau \gg 1$. Fig. 4 shows the dispersion of the dielectric constant versus $\omega\tau$. In the same plot, the conductivity crosses over from its low frequency value to a power law behavior, $\sigma(\omega\tau \gg 1) \propto (\omega\tau)^{1-b}$, at intermediate frequencies.

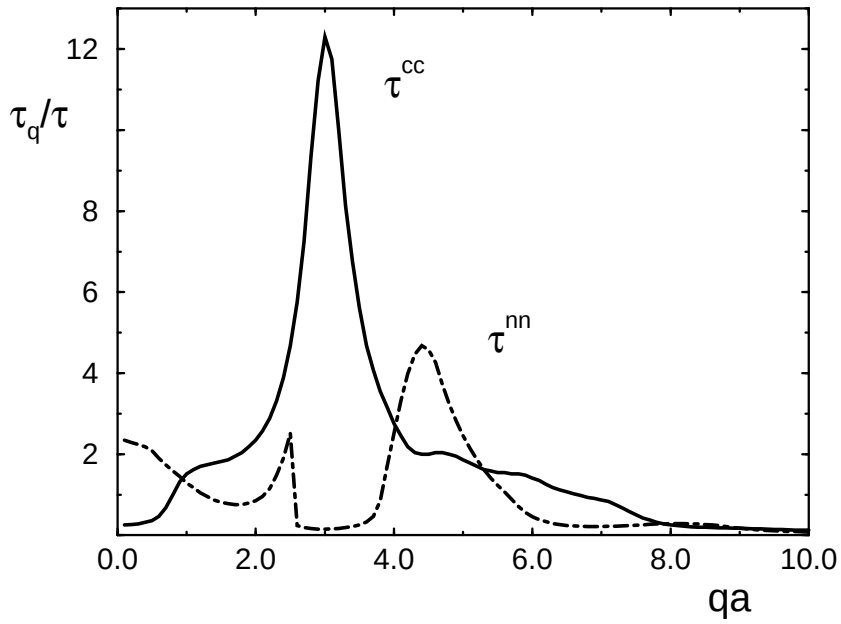

Figure 3: Wave vector dependent factors of the α–relaxation times τ_q^{nn}/τ and τ_q^{cc}/τ.

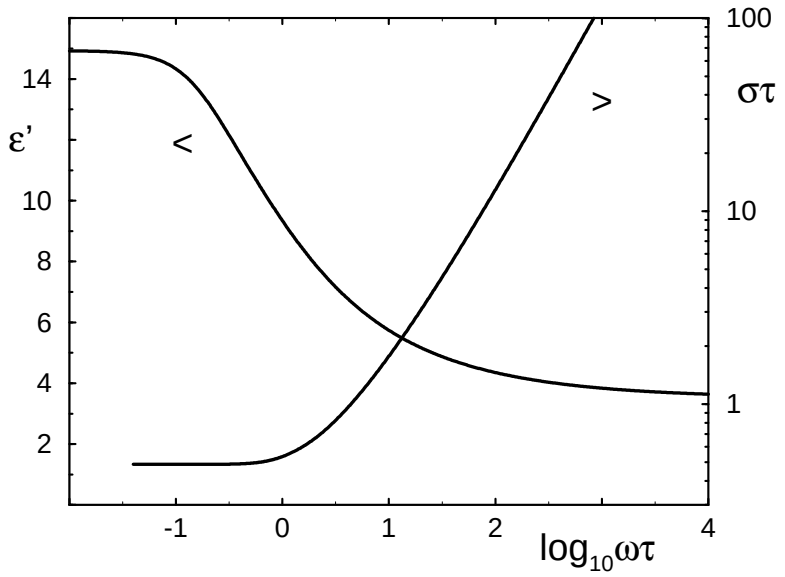

Figure 4: Scaled conductivity $\sigma\tau$ and real part of the dielectric constant ε versus $\omega\tau$.

Discussion

The mixed salt CKN [40% $Ca(NO_3)_2$- 60% KNO_3] is a well studied glassforming melt; see [7,8] and references therein. Its dynamics in a wide temperature range has been studied by neutron [7] and by depolarized light scattering [8]. In the latter work it was found that the exponent parameter $\lambda \approx 0.85$ describes the dynamics in an intermediate time window. These findings lead to the choice of parameters in our model reproducing this λ–value. This assures that the asymptotic dynamics in the intermediate time window is described by the correct asymptotic master function exhibiting, for example, the von Schweidler asymptote of Eq. (4) or Fig. 4.

The wave vector dependent prefactors, like f_q, h_q and τ_q, are strongly coupled to the structural input as specified by our model and discussed in the previous chapter. It cannot be expected that the simple model reproduces these amplitudes quantitatively. However, the variations of the α–amplitude f_q^{cc} and relaxation time τ_q^{cc} in phase with S_q^{cc} and of the critical amplitude h_q^{cc} out of phase with it, are expected to be general findings applicable to molten salts. The corresponding variations in the mass–density quantities shown in Fig. 1 have been found in MCT calculations for different simple liquids [2,6]. They have been compared to dynamic light scattering spectra in colloidal suspensions; general agreement with errors of the order of 15% was observed [9]. Neutron scattering from CKN measures a combination of charge– and mass–density fluctuations determined by the different atomic neutron scattering cross sections. Our findings of peaks in the α–amplitudes and in the α–times at the wave vectors, q_c and q_n, characterizing charge and density fluctuations in the equilibrium structure, are in qualitative agreement with the reported measurements [7]. The results show that charge ordering and local packing are the underlying mechanism.

Let us restate, that the increase of the time scales at peaks in the static structure factors is not a simple example of de Gennes narrowing and cannot be explained by short time sum rules but is a consequence of the MCT equations (1) [2]. Eqs. (1) do not include the short time dynamics and consequently violate the short time sum rules. The shown

variations result from the specific magnitudes of the coupling of different modes in the memory functions; the couplings are determined by S_q.

The MCT equations (1) correctly describe non–propagating and non–diffusive charge fluctuations in the long–wavelength limit (3). This is a consequence of screening in ionic melts which requires finite restoring forces for charge fluctuations even on long wavelengths. The generalized conductivity changes from a low frequency constant, $\sigma \propto 1/\tau$, to a power law behavior at large $\omega\tau$.

In a cursory search liquid glass transitions were located for different parameters in this model. The parameter of table I lead to a rather strong peak in the charge structure factor, S_q^{cc}. The origin of this is the large charge asymmetry z_2/z_2 =-3 which entails a corresponding concentration ratio due to the requirement of global neutrality. The overestimated charge oscillations lead to two special features in our results. First, the maxima in the q–dependent amplitudes of the charge fluctuations are quite pronounced. This prevents any quantitative comparisons with the neutron or light scattering data of [7,8]. This failure emphasizes that quantitative comparisons between MCT calculations for simple liquids and experimental data require appropriate microscopic models if non–universal features of the theory are tested; see [6,9]. Second, comparing Fig. 1 to the corresponding results for one–component liquids, shows that the frozen–in mass-density structure of the formed glass is similar but somewhat distorted. Inspection of other parameter values in this model reveals that another glassy structure becomes stable if the charge asymmetry is increased some more. The small stability of the studied glass to another amorphous structure is the origin of the large exponent parameter. This second glass differs in the frozen–in mass–density but not in the charge–density structure. A striking consequence of the proximity of the two glassy states is the splitting of the α–relaxation in $F_q^{nn}(t)$ for some wave vectors into two processes. This effect is indicated in Fig. 3, where the inverse α–peak position frequency jumps from one process to the other at $qa \approx$2.5. This phenomenon has been discussed in schematic MCT models [10] and will be studied further in this microscopic model.

Acknowledgments

Financial support from the Deutsche Forschungsgemeinschaft under contract Fu 309/1-1 is acknowledged.

References

1. J.P. Hansen and I.R. McDonald, *Theory of Simple Liquids*, 2nd edn. (Academic Press, London, 1986), p.364.
2. W. Götze and L. Sjögren, Rep. Prog. Phys. **55**, 241 (1992); and references therein.
3. L. Blum and J.S. Høye, J.Phys.Chem. **81**, 1311 (1977).
4. J.S. Thakur and J. Bosse, J.Non-Cryst.Solids **117/118**, 898 (1990).
5. J. Bosse and T. Munakata, Phys.Rev. **A 25**, 2763 (1982); L. Sjögren and F. Yoshida, J.Chem.Phys. **77**, 3703 (1982).
6. M. Fuchs, I. Hofacker and A. Latz, Phys.Rev. **A 45**, 898 (1992); and references therein.
7. F. Mezei, W. Knaak and B. Farago, Physica Scripta **T 49**, 363 (1987).
8. H.Z. Cummins, W.M. Du, M. Fuchs, W. Götze, S. Hildebrand, A. Latz, G. Li and N.J. Tao, Phys.Rev. **E 47**, 4223 (1993).
9. W. van Megen and S.M. Underwood, Phys.Rev. **E 49**, 4206 (1994).
10. M. Fuchs, W. Götze, I. Hofacker and A. Latz, J.Phys.:Condens.Matter **3**, 5047 (1991).